HHS Public Access

Author manuscript

Technol Cancer Res Treat. Author manuscript; available in PMC 2015 June 18.

Published in final edited form as:

Technol Cancer Res Treat. 2008 December ; 7(6): 449–456.

Design and Testing of a Simulation Framework for Dosimetric Motion Studies Integrating an Anthropomorphic Computational Phantom into Four-dimensional Monte Carlo

M. Riboldi, Ph.D.[1,*], **G. T. Y. Chen, Ph.D.**[2], **G. Baroni, Ph.D.**[1], **H. Paganetti, Ph.D.**[2], and **J. Seco, Ph.D.**[2]

[1]TBMLab, Department of Bioengineering, Politecnico di Milano University, P.za Leonardo da Vinci 32, 20133 Milano, Italy

[2]Department of Radiation Oncology, Massachusetts General Hospital and Harvard Medical School, 100 Blossom Street, Boston, MA 02114, USA

Abstract

We have designed a simulation framework for motion studies in radiation therapy by integrating the anthropomorphic NCAT phantom into a 4D Monte Carlo dose calculation engine based on DPM. Representing an artifact-free environment, the system can be used to identify class solutions as a function of geometric and dosimetric parameters. A pilot dynamic conformal study for three lesions (~ 2.0 cm) in the right lung was performed (70 Gy prescription dose). Tumor motion changed as a function of tumor location, according to the anthropomorphic deformable motion model. Conformal plans were simulated with 0 to 2 cm margin for the aperture, with additional 0.5 cm for beam penumbra. The dosimetric effects of intensity modulated radiotherapy (IMRT) vs. conformal treatments were compared in a static case. Results show that the Monte Carlo simulation framework can model tumor tracking in deformable anatomy with high accuracy, providing absolute doses for IMRT and conformal radiation therapy. A target underdosage of up to 3.67 Gy (lower lung) was highlighted in the composite dose distribution mapped at exhale. Such effects depend on tumor location and treatment margin and are affected by lung deformation and ribcage motion. In summary, the complexity in the irradiation of moving targets has been reduced to a controlled simulation environment, where several treatment options can be accurately modeled and quantified The implemented tools will be utilized for extensive motion study in lung/liver irradiation.

Keywords

Monte Carlo; 4D dosimetry; Computational phantom; Organ motion

[*]Corresponding Author: M. Riboldi, Ph.D., marco.riboldi@polimi.it.

Introduction

In the treatment of moving tumors, different strategies may be applied to mitigate the effects of breathing motion on external beam dose delivery. These include the irradiation of the internal target volume (ITV) (1), respiratory gating (2, 3) and tumor tracking (4–8). Such techniques entail an increasing level of complexity in terms of treatment planning and technology needed for accurate targetry. It is still unclear though what is the dosimetric gain in using complex motion mitigation strategies for different tumor location, size, motion amplitude. Furthermore, the level of geometrical uncertainty in targeting the tumor, due to setup error and residual motion, translates into the use of safety margins around the CTV. As a matter of fact, the potential benefit of one strategy over the other results from the complex interaction of multiple variables.

4D CT is a clinically available option to perform patient specific analysis, aiming at defining the best treatment modality in a case specific way (9, 10). Such analysis is labor intensive, involving target and normal tissue segmentation over multiple respiratory phases, the application of deformable registration techniques and extensive 4D planning (11). Furthermore, one has to deal with motion artifacts due to irregular breathing and/or inaccuracies in phase binning of 4D CT images (12, 13).

In this scenario, computational models may play a complementary role in providing insights into action thresholds. Several anthropomorphic computational models for radiation dosimetry have been developed since the 1960s, ranging from stylized to voxel-based models (14, 15). These latter have reached sub-millimeter anatomical detail relying on tomographic images of real subjects (15). Recent developments have extended the capabilities of computational models to incorporate 4D motion, namely respiration and heartbeat (16–18). These features make latest 4D anthropomorphic models extremely valuable for extensive dosimetric studies of the effects of motion.

Motion studies can be performed by integrating 4D models into a dose calculation engine. Monte Carlo emerges as the best solution, given the intrinsic accuracy, especially for low density materials and in presence of heterogeneities (19). This specifically applies to motion studies in the lung (20). The use of 4D Monte Carlo dose calculations for time dependent geometries, including variations in patient anatomy due to organ motion, has proven to be highly efficient (21–23). Moreover, 4D Monte Carlo has been shown to have the same computational time of a 3D dose calculation featuring the same statistical uncertainty (21).

Consequently, we applied Monte Carlo dose calculations on an anthropomorphic 4D computational patient model to understand the effects of motion on dose deposition. Our approach to 4D Monte Carlo dose calculation in patient data is described in detail in a previous publication (24). We extended the use of our 4D Monte Carlo calculation engine to integrate an anthropomorphic 4D computational phantom in a unique simulation framework. This represents a framework where the interactions of multiple variables can be conveniently modeled to quantify the dosimetric effects due to motion. The advantage of this approach is the availability of a controlled environment, where no inaccuracies in 4D CT acquisition, deformable registration and workload in data processing exist.

In this work, implementation and testing of the simulation framework for 4D Monte Carlo motion studies are reported. Conformal and IMRT treatment plans were generated and applied to coin size moving tumors in order to examine the accuracy in tracking and delivering dose in 4D. Dosimetric results were correlated to the anatomical changes induced by breathing, as a function of tumor motion, ribcage expansion and lung deformation.

Materials and Methods

4D Anthropomorphic Computational Model

NCAT (NURBS-based Cardiac-Torso) (17) is a spline-based anthropomorphic model created on the Visible Human Data-set (25). It includes a spline-based description of 3D human anatomy and dynamic 4D modeling of breathing (18) and heartbeat (16). The computational model can be used to generate 4D attenuation and/or activity medical images. Hereafter, we will focus on the use of NCAT to obtain artificial 4D CT images for radiotherapy planning studies.

In the standard NCAT release, the user can edit functional variables that control respiration and heart pulse, in order to generate deformable 4D CT models according to specific criteria (18). The main control variables include:

- Motion option: beating heart only/respiration only/combined mode
- Maximum diaphragm motion in the superior-inferior (SI) direction
- Maximum anterior-posterior (AP) expansion of the chest wall applies to motion studies in the lung (20).

Though the spline-based representation can provide a continuous model in space and time, the spatial resolution and phase binning of NCAT-generated 4D CT images can be adjusted. Spherical tumors of arbitrary location and size can be inserted into the NCAT 4D CT dataset, and contours of all organs and a deformable registration map can be extracted from the spline-based representation (Figure 1) (26).

4D Monte Carlo Dose Calculation

According to the approach proposed by Vanderstraeten *et al*. (27), 14 tissue subsets (materials) were utilized for Monte Carlo dose calculations. In our case, stoichiometric calibration was not necessary as density values for each voxel were provided by the NCAT model (28). Table I reports the properties of the 14 materials used for Monte Carlo dose calculations.

Monte Carlo dose calculation was done in three steps (24):

a. transport of electron and photons from the electron target to the flattening filter, performed with EGSnrc (29). The VARIAN 2100C/D treatment head was modeled based on manufacturer's information, in order to characterize the beam as a phase space distribution at the level of the flattening filter

b. transport of electrons and photons from the flattenning filter to after the MLC (multileaf collimator) using the variance reduction method published by Siebers *et*

al. (30). The method was expanded to incorporate the variations in the MLC and jaws during beam delivery or between different beams (24). This represents an efficient method of transporting photons through MLC/jaws and accounts for beam hardening and tongue-and-groove effect by using multiple Compton scatter in the MLC/jaws medium. The Compton scatter is sampled based upon the total thickness of MLC traversed. Pair production and electron interaction within the MLC are ignored.

c. Simulation of patient dose deposition using the DPM algorithm (31). DPM was used in favor of EGSnrc because it allows a more time efficient computation of dose in a patient/phantom geometry. The standard DPM parameters were used in the DPM simulations and the time variations were accounted for using a 4D CT data set (24). DPM and EGSnrc were benchmarked against each other showing agreement to within 1%. The various Monte Carlo algorithms used separately in either of the two methods were extensively studied by Kawarakow *et al*. (32).

Step (a) using EGSnrc software is only performed once during the commissioning of the Monte Carlo code to the linac present at our hospital. It is then unchanged for all the simulations of IMRT or non-IMRT field with Monte Carlo. Steps (b) and (c) are performed for all simulations of IMRT fields used in the present manuscript. The statistical uncertainty was calculated using the method of Walters *et al*. (33). The uncertainty in the present results are, for the target area approximately, 3% per beam, which corresponds to an overall uncertainty of below 2%.

Conformal Study

Three 4D anthropomorphic computational models were generated with NCAT. The spatial resolution of the resulting 4D CT images was set to 1.5625 mm (256 × 256 × 256 voxels). The same input parameters were applied to define breathing: 4 cm diaphragm motion and 2 cm chest wall expansion. This allowed us to test the implemented simulation framework in a case with large motion. The respiratory cycle was binned into 10 phases, with the exhale phase encompassing 60% of the total duration.

The models differed in the location of the tumor (~ 2.0 cm): three spherical lesions (LOW, MED, UP) were placed in the right lung (Figure 2). Given the spatial resolution of the generated 4D CT images, the lesions resulted in 12–14 voxels thick spherical objects. Tumor motion changed according to the motion model implemented in NCAT as a function of tumor location. Though the lung is modeled as a deformable object, the spherical lesion is assumed as a rigid object (18), being the motion defined by the center of mass. The peak to peak motion in the SI direction measured 3.8 cm, 2.8 cm, and 1.2 cm for the LOW, MED, and UP lesion, respectively. The corresponding motion amplitude in the AP direction was 0.9 cm, 0.9 cm, and 0.2 cm, correspondingly.

A conformal study was performed with Monte Carlo dose calculations, assuming a prescription dose of 70 Gy (95% coverage). The beam arrangement included 6 beams (0°, 22°, 180°, 228°, 270°, 334°) as shown in Figure 2. Beam weights were optimized at 50% inhale (phase 3).

Tumor tracking was simulated for each 4D phantom, relying on the NCAT breathing model to shift the beams in order to follow tumor motion over the respiratory cycle. Monte Carlo dose calculations were performed separately on each phase, considering $5 \cdot 10^7$ simulated photons ($5 \cdot 10^8$ total). The number of photons was selected to achieve less than 3% error in the dose calculation per beam in the target area, as specified in the previous section. Conformal plans were simulated with different margins added to the GTV: 0 cm, 1 cm, 2 cm. An additional 0.5 cm margin was applied to account for beam penumbra. The resulting dose distributions were mapped to the exhale phase as described in the previous section. The composite 4D dose allowed us to quantify the dosimetric effects of tumor tracking as a function of the applied margin. The rationale of using different margins in this study was to investigate and quantify the effect of rigid tumor motion vs. lung deformation on target coverage and normal lung irradiation.

Finally, ideal respiratory gating was simulated through the calculated dose distribution at exhale.

IMRT Case

The implemented simulation framework was used for Monte Carlo dose calculations in IMRT on a static case. This was obtained by making use of optimized MLC sequences calculated by a commercial treatment planning software. The extension of our 4D Monte Carlo framework to IMRT delivery is straightforward, as the dose mapping procedure applied in the conformal study is independent of the simulated irradiation technique. The same applies to accounting for variable density values in the lung as a function of the breathing phase: one can easily overwrite density values in any structure relying on 4D NCAT segmentation. On the other hand, potential interplay effects between organ motion and leaf motion (34) are currently not considered in our model.

The LOW lesion at exhale with 0 cm PTV margin was selected for Monte Carlo IMRT dose calculations. The same additional margin for beam penumbra used in the dynamic conformal study was applied. The NCAT generated 3D CT images were converted into the DICOM format and imported into XiO® treatment planning (CMS Inc.). This latter was used to generate optimized leaf-sequence for the MLC in five beams (0°, 180°, 228°, 270°, 334°). The MLC leaf-sequence files, featuring 6–12 segments for each beam, were then exported to the Monte Carlo dose calculation engine. The conversion from DICOM plan obtained using the XiO® treatment planning system to Monte Carlo was performed using the MATLAB® toolbox, which reads DICOM format. A total number of $5 \cdot 10^7$ photons were simulated for IMRT dose calculations.

Results and Discussion

Conformal Study

Monte Carlo dose calculation takes approximately under 1 hour of computational time per phase to achieve 3% error per beam in PTV dose prediction. Figure 3 depicts an exemplifying dynamic sequence of conformal dose distributions over the breathing cycle.

Dose volume histograms (DVHs) for the same tumor tracking case are shown in Figure 4. Results show dosimetric variations as a function of the breathing phase. Though accurate geometric tracking was achieved, as shown in Figure 3, target underdosage at inhale and overdosage at exhale were found (Figure 4).

Figure 5 shows target coverage as a function of margin for the three lesions, where the composite dose distribution over the breathing cycle is mapped to the exhale phase. With increasing margin the influence of the tumor location (LOW to UP) on the motion DVH becomes more pronounced. Target underdosage was highlighted for 1 cm and 2 cm margin, ranging from 1.58 Gy (LOW lesion, 2 cm margin) to 3.67 Gy (LOW lesion, 1 cm margin); results are expressed in terms of variation in the dose delivered to 95% of the target volume (D95).

Ideal tumor tracking on a rigidly moving tumor in the lung results in perfect target coverage when no margin is used. The same conclusion does not hold when a non zero margin is applied, due to the deformable anatomy of the lung (Figure 5). As a matter of fact, margins are a geometric concept that is used to define the aperture in order to cover a volume encompassing the tumor. When deformable anatomy is involved, the aperture defined on a specific breathing phase includes voxels of normal tissue that will be moving in or out, according to the local amount of deformation. Therefore, though one can effectively track over the breathing cycle any geometric volume around the tumor, dose coverage is not ensured for each single voxel included in the original target. Figure 5 also shows that such effect is dependent on tumor location (*i.e.*, motion amplitude) and the applied margin. The maximum variation was measured for the LOW lesion, *i.e.*, where deformation is larger. Target underdosage was found to be higher for the 1 cm than the 2 cm margin. This is consistent with the observation that, when the margin is wide enough, lung deformation has reduced effects, as the aperture effectively includes the portion of lung volume that is deforming the most. When comparing the target dose for different margins, results may be affected by the uncertainties in DVH estimation, that are larger for the zero margin case compared to 1 cm and 2 cm margin. Though this was not quantified in our simulations, results are in keeping with the anatomo-physiological changes induced by breathing in the anthropomorphic phantom, indicating that the effect has a significantly smaller magnitude.

Figure 6 compares tumor tracking and respiratory gating showing DVHs for the right lung for the LOW and UP lesion. It is worth stressing that these results were obtained considering constant lung density over the breathing cycle. Recent studies show that such approximation results in minor effects if compared to motion and heterogeneities correction (20, 35). Normal lung DVHs illustrate that tracking has a dosimetric advantage vs. gating, at least in a large motion case. This can be explained by the fact that the radiation beam intersects the normal lung at different locations when tumor tracking is performed, thus locally reducing dose deposition in the healthy lung. Such effect was also found to be dependent on the applied margin, with an increasing trend for larger margins. Figure 6 shows that the actual gain is negligible as long as the margin can be reduced to a minimum (ideally zero). This should be accurately considered, as the technological and methodological effort to reduce the uncertainties in tumor tracking is definitely of higher magnitude than the one needed for

respiratory gating. On the other hand, tumor tracking can significantly increase the duty cycle, thus reducing the overall treatment time in the irradiation of a moving target.

The change in beam weight to ensure optimal target coverage over the breathing cycle was also investigated. Results for the beam at 0° are shown in Figure 7. Variations in optimal beam weights over the breathing cycle are highly dependent on the amount of bone tissue within the aperture, especially for lesions in the medium/lower lung when small margins are applied (Figures 7, 8). With larger apertures (1–2 cm margin) bone tissue variations were averaged out, and beam weights showed a higher correlation with the amount of lung tissue. Therefore, beam weight changes are sensitive to tumor location on one hand, and ribcage bony structures moving in and out of the aperture on the other. Consequently, deriving a reliable model of weight variations over the breathing cycle is not a trivial task, as anatomy variations need to be site specifically quantified. Conversely, this emphasizes the need for an accurate simulation framework where such effects can be conveniently and quantitatively studied.

IMRT Case

The 3D dose distribution when IMRT was simulated is depicted in Figure 9, compared to the corresponding 3D conformal case.

Figure 10 shows the variations in the dose gradient outside of the GTV. The advantage of IMRT vs. 3D CRT is visible from the considerably steeper DVH for the GTV (thick lines in Figure 10). Also, concentric volumes encompassing the GTV highlight a reduction in dose deposition, signifying higher conformality in the dose distribution.

Conclusion

A simulation framework comprising a 4D anthropomorphic computational model and a 4D Monte Carlo dose calculation engine has been implemented. This study shows that the simulation framework can model tumor tracking in deformable anatomy with high accuracy. Furthermore, the absolute dosimetry provided by 4D Monte Carlo dose calculations effectively quantifies variations due to anatomical structures moving in and out of the radiation beam pathway. The implemented tools have been applied to a dynamic conformal study for three lesions in the right lung.

The complexity in the irradiation of moving targets has been reduced to a controlled 4D simulation environment for dosimetric motion studies. Anatomical changes due to breathing need to be carefully considered even though perfect tumor tracking can be achieved. When large motion occurs, the anatomical structures moving in and out of the radiation beam pathway alter dose deposition over the breathing cycle. The dosimetric advantages of tumor tracking vs. respiratory gating in normal lung irradiation seem negligible, when high accuracy in tumor localization leads to small safety margins.

The implemented 4D Monte Carlo tools have been successfully tested and will be applied for extensive motion study in lung/liver irradiation. Future developments will extend the

implemented tools to include lung density variations and particle beam Monte Carlo dose calculations.

Acknowledgments

The work is partly supported by NCI/NIH R01-CA111590. We also acknowledge the Progetto Rocca foundation for the support.

Abbreviations

3D	Three-dimensional
4D	Four-dimensional
AP	Anterior posterior
CRT	Conformal radiotherapy
CT	Computed tomography
CTV	Clinical target volume
DVH	Dose volume histogram
GTV	Gross target volume
IMRT	Intensity modulated radiotherapy
ITV	Internal target volume
MLC	Multi-leaf collimator
NCAT	NURBS-based cardiac torso
NURBS	Non uniform rational B-splines
PTV	Planned target volume
SI	Superior inferior

References

1. Liu HH, Balter P, Tutt T, Choi B, Zhang J, Wang C, Chi M, Luo D, Pan T, Hunjan S, Starkschall G, Rosen I, Prado K, Liao Z, Chang J, Komaki R, Cox JD, Mohan R, Dong L. Assessing respiration-induced tumor motion and internal target volume using four-dimensional computed tomography for radiotherapy of lung cancer. Int J Radiat Oncol Biol Phys. 2007; 68:531–540. [PubMed: 17398035]
2. Jiang SB. Radiotherapy of mobile tumors. Semin Radiat Oncol. 2006; 16:239–248. [PubMed: 17010907]
3. Keall PJ, Vedam S, George R, Bartee C, Siebers J, Lerma F, Weiss E, Chung T. The clinical implementation of respiratory-gated intensity-modulated radiotherapy. Med Dosim. 2006b; 31:152–162. [PubMed: 16690456]
4. Neicu T, Shirato H, Seppenwoolde Y, Jiang SB. Synchronized moving aperture radiation therapy (SMART): average tumour trajectory for lung patients. Phys Med Biol. 2003; 48:587–598. [PubMed: 12696797]
5. D'Souza WD, Naqvi SA, Yu CX. Real-time intra-fraction-motion tracking using the treatment couch: a feasibility study. Phys Med Biol. 2005; 50:4021–4033. [PubMed: 16177527]
6. Gibbs IC. Frameless image-guided intracranial and extracranial radiosurgery using the Cyberknife robotic system. Cancer Radiother. 2006; 10:283–287. [PubMed: 16859948]

7. Keall PJ, Cattell H, Pokhrel D, Dieterich S, Wong KH, Murphy MJ, Vedam SS, Wijesooriya K, Mohan R. Geometric accuracy of a real-time target tracking system with dynamic multileaf collimator tracking system. Int J Radiat Oncol Biol Phys. 2006a; 65:1579–1584. [PubMed: 16863935]
8. Shirato H, Shimizu S, Kitamura K, Onimaru R. Organ motion in image-guided radiotherapy: lessons from real-time tumor-tracking radiotherapy. Int J Clin Oncol. 2007; 12:8–16. [PubMed: 17380435]
9. Engelsman M, Rietzel E, Kooy HM. Four-dimensional proton treatment planning for lung tumors. Int J Radiat Oncol Biol Phys. 2006; 64:1589–1595. [PubMed: 16580508]
10. Rietzel E, Liu AK, Doppke KP, Wolfgang JA, Chen AB, Chen GTY, Choi NC. Design of 4D treatment planning target volumes. Int J Radiat Oncol Biol Phys. 2006; 66:287–295. [PubMed: 16904528]
11. Kang Y, Zhang X, Chang JY, Wang H, Wei X, Liao Z, Komaki R, Cox JD, Balter PA, Liu H, Zhu XR, Mohan R, Dong L. 4D Proton treatment planning strategy for mobile lung tumors. Int J Radiat Oncol Biol Phys. 2007; 67:906–914. [PubMed: 17293240]
12. Chen GTY, Kung JH, Beaudette KP. Artifacts in computed tomography scanning of moving objects. Semin Radiat Oncol. 2004; 14:19–26. [PubMed: 14752730]
13. Mutaf YD, Antolak JA, Brinkmann DH. The impact of temporal inaccuracies on 4DCT image quality. Med Phys. 2007; 34:1615–1622. [PubMed: 17555243]
14. Caon M. Voxel-based computational models of real human anatomy: a review. Radiat Environ Biophys. 2004; 42:229–235. [PubMed: 14730450]
15. Zaidi H, Xu XG. Computational anthropomorphic models of the human anatomy: the path to realistic Monte Carlo modeling in radiological sciences. Annu Rev Biomed Eng. 2007; 9:471–500. [PubMed: 17298237]
16. Segars WP, Lalush DS, Tsui BMW. A realistic spline-based dynamic heart phantom. IEEE Trans Nucl Sci. 1999; 46:503–506.
17. Segars, WP. PhD dissertation. The University of North Carolina; 2001. Development of a new dynamic NURBS-based cardiac-torso (NCAT) phantom.
18. Garrity JM, Segars WP, Knisley SB, Tsui BMW. Development of a dynamic model for the lung lobes and airway tree in the NCAT phantom. IEEE Trans Nucl Sci. 2003; 50:378–383.
19. Seco J, Adams E, Bidmead M, Partridge M, Verhaegen F. Head-and-neck IMRT treatments assessed with a Monte Carlo dose calculation engine. Phys Med Biol. 2005; 50:817–830. [PubMed: 15798257]
20. Rosu M, Chetty IJ, Tatro DS, Ten Haken RK. The impact of breathing motion versus heterogeneity effects in lung cancer treatment planning. Med Phys. 2007; 34:1462–1473. [PubMed: 17500477]
21. Keall PJ, Siebers JV, Joshi S, Mohan R. Monte Carlo as a four-dimensional radiotherapy treatment-planning tool to account for respiratory motion. Phys Med Biol. 2004; 49:3639–3648. [PubMed: 15446794]
22. Paganetti H, Jiang H, Adams JA, Chen GTY, Rietzel E. Monte Carlo simulations with time-dependent geometries to investigate effects of organ motion with high temporal resolution. Int J Radiat Oncol Biol Phys. 2004; 60:942–950. [PubMed: 15465213]
23. Paganetti H, Jiang H, Trofimov A. 4D Monte Carlo simulation of proton beam scanning: modelling of variations in time and space to study the interplay between scanning pattern and time-dependent patient geometry. Phys Med Biol. 2005; 50:983–990. [PubMed: 15798270]
24. Seco J, Sharp GC, Wu Z, Gierga DP, Buettner F, Paganetti H. Dosimetric impact of motion in free-breathing and gated lung radiotherapy: a 4D Monte Carlo study of intrafraction and interfraction effects. Med Phys. 2008; 35:356–366. [PubMed: 18293590]
25. Spitzer VM, Whitlock DG. The Visible Human Dataset: the anatomical platform for human simulation. Anat Rec. 1998; 253:49–57. [PubMed: 9605360]
26. Mair BA, Gilland DR, Sun J. Estimation of images and nonrigid deformations in gated emission CT. IEEE Trans Med Imaging. 2006; 25:1130–1144. [PubMed: 16967799]
27. Vanderstraeten B, Chin PW, Fix M, Leal A, Mora G, Reynaert N, Seco J, Soukup M, Spezi E, De Neve W, Thierens H. Conversion of CT numbers into tissue parameters for Monte Carlo dose calculations: a multi-centre study. Phys Med Biol. 2007; 52:539–562. [PubMed: 17228104]

28. Schneider W, Bortfeld T, Schlegel W. Correlation between CT numbers and tissue parameters needed for Monte Carlo simulations of clinical dose distributions. Phys Med Biol. 2000; 45:459–478. [PubMed: 10701515]
29. Kawrakow I. Accurate condensed history Monte Carlo simulation of electron transport: I. EGSnrc, the new EGS4 version. Med Phys. 2000; 27:485–498. [PubMed: 10757601]
30. Siebers JV, Keall PJ, Kim JO, Mohan R. 2002 A method for photon beam Monte Carlo multileaf collimator particle transport. Phys Med Biol. 2002; 47:3225–3249. [PubMed: 12361220]
31. Sempau J, Wilderman SJ, Bielajew AF. DPM, a fast, accurate Monte Carlo code optmized for photon and electron radiotherapy treatment planning dose calculations. Phys Med Biol. 2000; 45:2263–2291. [PubMed: 10958194]
32. Kawrakow I, Bielajew AF. On the condensed history technique for electron transport. Nucl Instr Meth. 1998; 142B:253–280.
33. Walters BR, Kawrakow I, Rogers DW. History by history statistical estimators in the BEAM code system. Med Phys. 2002; 29:2745–2752. [PubMed: 12512706]
34. Seco J, Sharp GC, Turcotte JC, Gierga DP, Bortfeld T, Paganetti H. Effects of organ motion on IMRT treatments with segments of few monitor units. Med Phys. 2007; 34:923–934. [PubMed: 17441238]
35. McGurk R, Riboldi M, Seco J, Paganetti H, Wolfgang J, Chen G. Impact of tumor motion and size in the irradiation of moving tumors in step-and-shoot IMRT: A NCAT based 4D Monte Carlo simulation study. Med Phys. 2008; 35:2798.

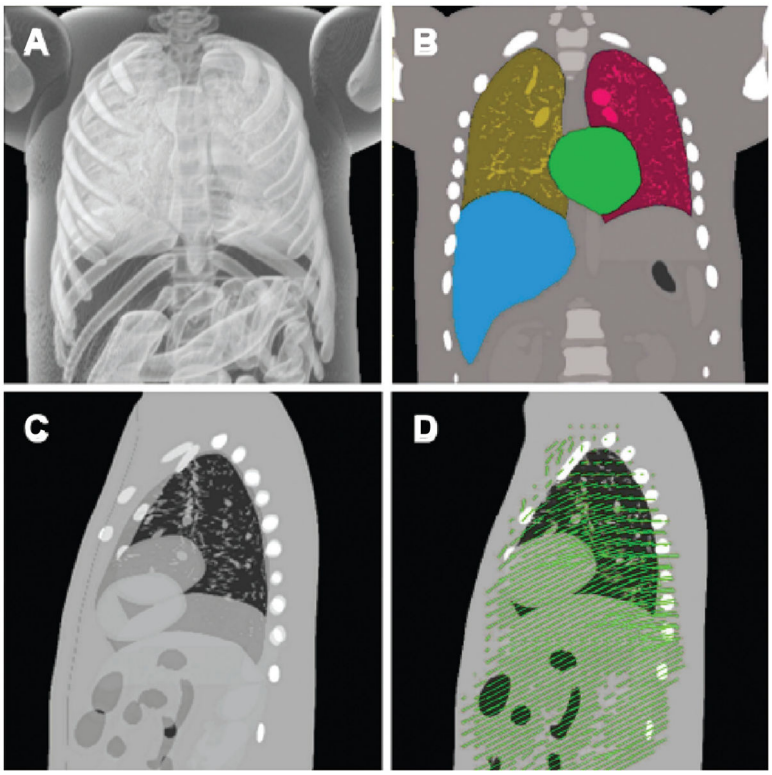

Figure 1.

Panel **A**: NCAT based 3D rendering at exhale, where the anatomical details inside the lung are visible. Panel **B**: segmented NCAT model showing the right/left lung, heart, and liver. Panel **C**: sagittal view with exhale and inhale superimposed in transparency. Panel **D**: deformation vector field mapping exhale to inhale.

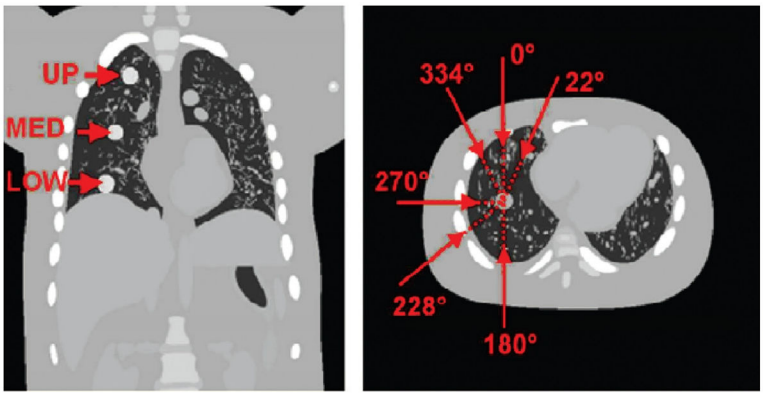

Figure 2.

Anatomical location of the three lesions (LOW, MED, UP) located in the right lung (*left panel*). Only one lesion was used for a given simulation setup. The right panel shows the exemplifying beam arrangement for the conformal study.

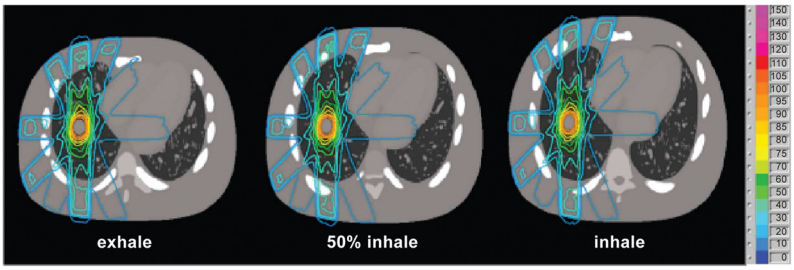

Figure 3.

Monte Carlo dose distribution at exhale, 50% inhale, and inhale during tumor tracking with no additional margin except for penumbra (LOW lesion).

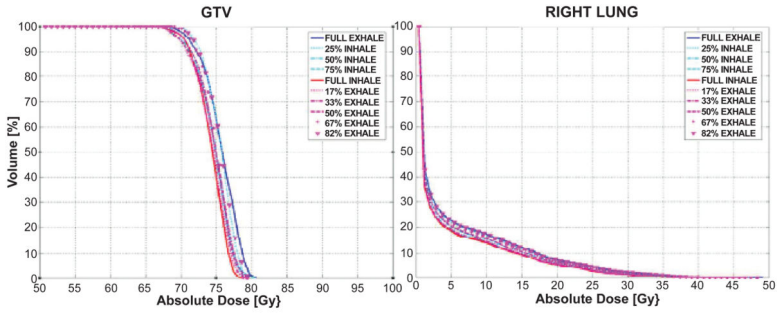

Figure 4.
DVHs for GTV and right lung (0 cm margin) over the breathing cycle for the LOW lesion.

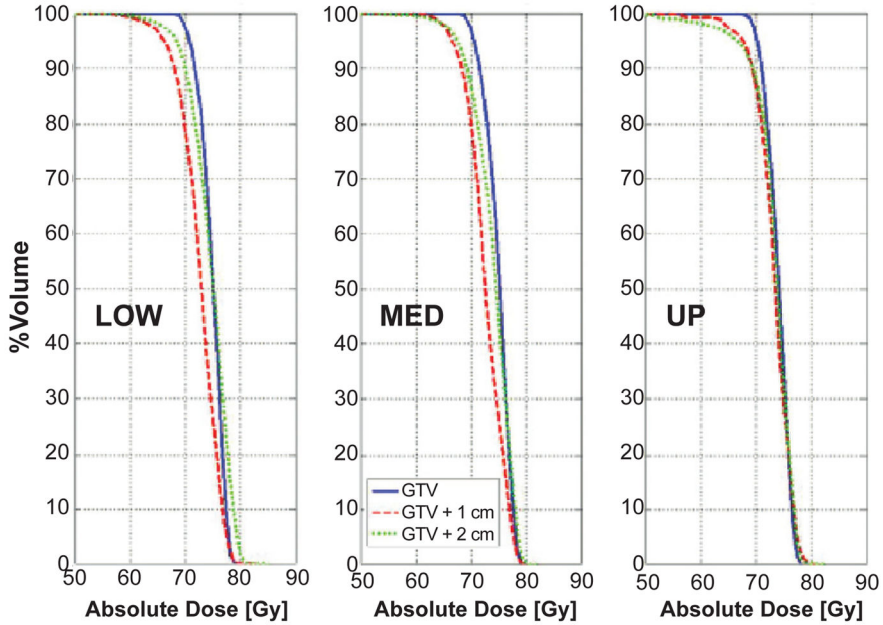

Figure 5.

DVHs of 4D Monte Carlo dose calculations over the breathing cycle, mapped at exhale. Results are shown as a function of tumor location and margin.

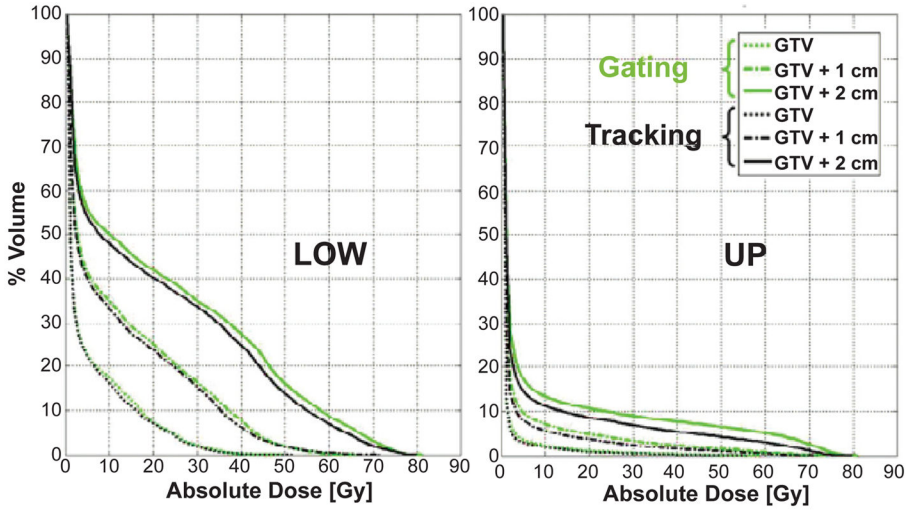

Figure 6.

Normal tissue irradiation (right lung) for the LOW and UP lesion, where respiratory gating is compared to tumor tracking.

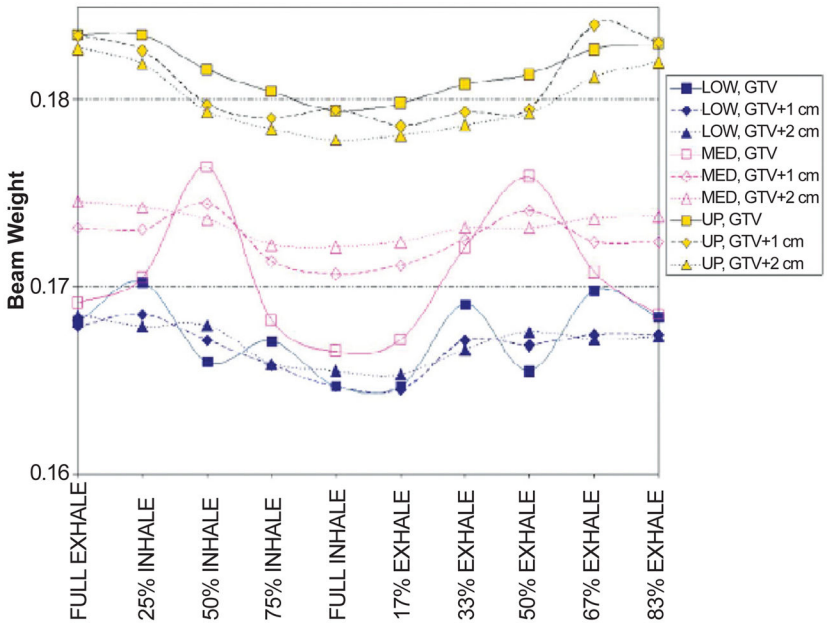

Figure 7.

Beam weight variation over the breathing cycle for the beam at 0° (AP) as a function of tumor location (LOW, MED, UP) and margin (0, 1, 2 cm).

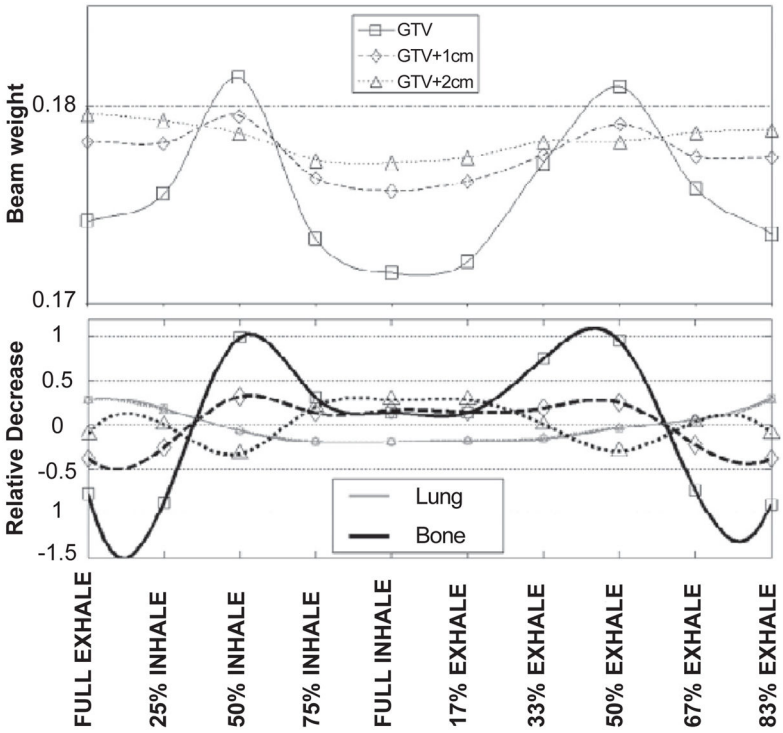

Figure 8.

Beam weight variation for the MED lesion as a function of margin for the beam at 0° (upper panel); the lower panel shows the relative decrease in lung/bone tissue in the aperture with respect to the average value over the breathing cycle.

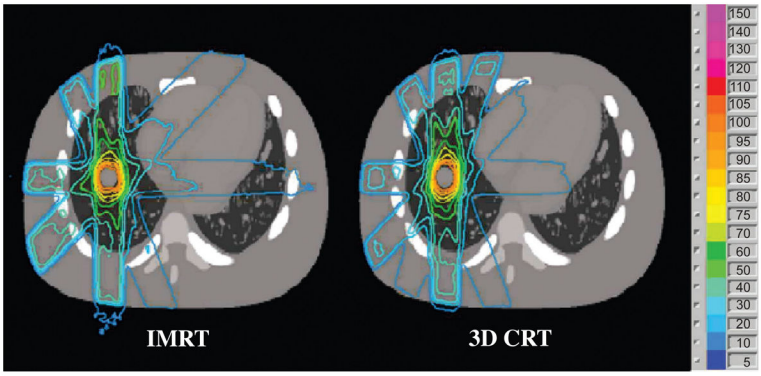

Figure 9.
IMRT vs. 3D conformal (3D CRT) dose distribution.

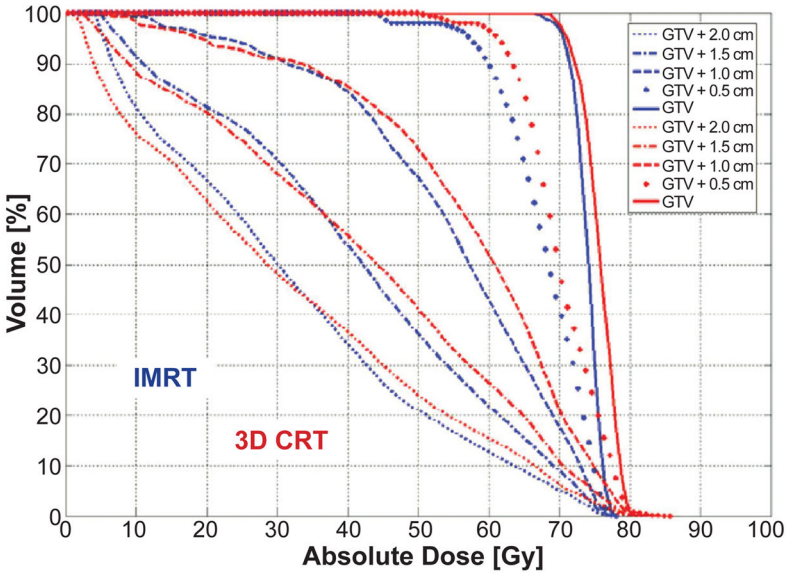

Figure 10.

DVHs of multiple volumes encompassing the GTV for IMRT (blue) and 3D CRT (red) at exhale.

Table I

Material composition and properties for Monte Carlo dose calculations.

Material	Composition							Z	A [Da]	Medium toH20 Stopping Power	Density Range [g/cc]	
	H	C	N	O	P	Ca	Ar				Min	Max
1	-	0.000	0.784	0.211	-	-	0.005	7.262	14.548	1.110	$-\infty$	0.095
2	0.130	0.105	0.031	0.749	0.002	-	-	6.999	13.872	0.996	0.095	0.879
3	0.117	0.697	0.001	0.189	-	-	-	5.826	11.544	0.995	0.879	0.997
4	0.107	0.120	0.024	0.755	0.001	-	-	7.050	13.996	1.013	0.997	1.057
5	0.097	0.465	0.025	0.355	0.019	0.041	-	7.010	13.951	1.024	1.057	1.152
6	0.089	0.424	0.027	0.365	0.030	0.064	-	7.479	14.910	1.040	1.152	1.247
7	0.075	0.357	0.031	0.384	0.049	0.106	-	8.355	16.695	1.054	1.247	1.342
8	0.066	0.314	0.033	0.396	0.061	0.131	-	8.886	17.779	1.068	1.342	1.437
9	0.059	0.277	0.035	0.406	0.071	0.154	-	9.348	18.721	1.079	1.437	1.533
10	0.052	0.245	0.037	0.414	0.080	0.173	-	9.753	19.548	1.090	1.533	1.628
11	0.046	0.216	0.039	0.422	0.087	0.191	-	10.111	20.279	1.100	1.628	1.723
12	0.041	0.190	0.040	0.429	0.094	0.206		10.430	20.930	1.117	1.723	1.818
13	0.036	0.167	0.042	0.435	0.101	0.220		10.716	21.513	1.125	1.828	1.913
14	0.044	0.200	0.054	0.559	0.132	0.029		8.657	17.403	1.129	1.914	$+\infty$